A UNIFIED HYBRID MODE ANALYSIS FOR PLANAR TRANSMISSION LINES WITH MULTILAYER ISOTROPIC/ANISOTROPIC SUBSTRATES

J-24

R. R. Mansour and R. H. MacPhie

Department of Electrical Engineering
University of Waterloo
Waterloo, Ontario, Canada N2L 3G1

ABSTRACT

A unified hybrid mode analysis is presented for determining the propagation characteristics of multiconductor multilayer planar transmission lines. The analysis employs the conservation of complex power technique, and the emphasis is on numerical efficiency and simplicity. Numerical results, for finline and microstrip configurations, aim at the clarification of the effects of the metallization thickness, dielectric anisotropy and substrate mounting grooves.

INTRODUCTION

During the past several years, a variety of techniques have been published for the characterization of planar transmission lines, techniques wherein there has been always a compromise between accuracy and numerical efficiency. In many cases, simplified approximations were introduced to achieve a good numerical efficiency at the expense of the accuracy. For example, most published techniques do not take into account the effect of the substrate mounting groove. Elsewhere, numerous results are reported for idealized structures with zero metallization thickness.

With the increasing complexity of microwave and millimeter-wave circuit design, attention has been directed in recent years to generalized approaches that can treat a variety of planar transmission lines with more complicated configurations. Thus, in developing a new technique the "generalization" has become another challenging factor to be considered in addition to the accuracy and numerical efficiency.

Among the published rigorous techniques are the spectral domain technique and the singular integral equation technique which have been extended in [1],[2] to analyze multiconductor planar transmission lines. Although these techniques have a very good numerical efficiency, they do not include the effects of metallization thickness and substrate mounting grooves. Very recently, an approach based on the mode matching technique has been presented in [3] to calculate the propagation constant, and extended in [4] to calculate the characteristic impedance. This approach however has a very poor numerical efficiency. Moreover in view of the study given in [5] on the convergence of the modal analysis numerical solution, the mode matching formulation used in this approach may fail to provide accurate results for structures with relatively small metallization thickness.

In this contribution, we present a hybrid mode approach for evaluating the propagation constants of the dominant and the higher order modes and the characteristic impedance for planar transmission lines with multiconductor and multilayer isotropic/anisotropic substrates. Besides the versatility and flexibility of this approach in treating complicated structures, it is numerically efficient and it includes the effects of the metallization thickness and substrate mounting grooves.

FORMULATION OF THE PROBLEM

A generalized planar guiding structure is shown in Fig. 1. It consists of an arbitrary number of metallic strips deposited on the various interfaces of a multilayer isotropic/anisotropic dielectric substrate. The hybrid nature of the electromagnetic field in this structure, can be attributed to the coupling between LSE and LSM modes. By considering the propagation to take place along the y-direction, the discontinuities at the various vertical planes serve to couple the LSE and LSM modes and the hybrid modes are formed as a result of the repeated reflections of LSE and LSM modes from the short-circuited ends and the discontinuities.

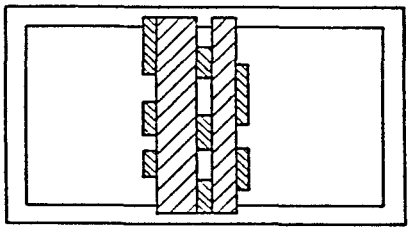

Fig. 1. A generalized planar guiding structure.

The first step in the analysis uses the conservation of complex power technique CCPT to treat the problem of scattering at the the N-furcated waveguide discontinuity shown in Fig. 2 for LSE and LSM excitation. Because of the coupling between the LSE and LSM modes the basic three matrices $\mathbf{H}$, $\mathbf{P_A}$,$\mathbf{P_B}$ defined in the CCPT formulation [5],[6] can be written as:

This work was supported by the Natural Sciences and Engineering Research Council (NSERC), Ottawa, Canada, under Grant A-2178.

0149-645X/87/0000-0341$01.00 © 1987 IEEE

$$\mathbf{H} = \begin{bmatrix} \mathbf{H}_1^{hh} & \mathbf{H}_1^{he} & \mathbf{H}_2^{hh} & \cdots\cdots & \mathbf{H}_N^{hh} & \mathbf{H}_N^{he} \\ \mathbf{H}_1^{eh} & \mathbf{H}_1^{ee} & \mathbf{H}_2^{eh} & \cdots\cdots & \mathbf{H}_N^{eh} & \mathbf{H}_N^{ee} \end{bmatrix}. \quad (1)$$

$$\mathbf{P}_A = \begin{bmatrix} \mathbf{P}_A^h & \mathbf{0} \\ \mathbf{0} & \mathbf{P}_A^e \end{bmatrix}, \quad \mathbf{P}_B = \begin{bmatrix} \mathbf{P}_{B1}^h & \mathbf{0} & \mathbf{0} & \cdots & \mathbf{0} & \mathbf{0} \\ \mathbf{0} & \mathbf{P}_{B1}^e & \mathbf{0} & \cdots & \mathbf{0} & \mathbf{0} \\ \mathbf{0} & \mathbf{0} & \mathbf{P}_{B2}^h & \cdots & \mathbf{0} & \mathbf{0} \\ \cdots & \cdots & \cdots & \cdots & \cdots & \cdots \\ \mathbf{0} & \mathbf{0} & \mathbf{0} & \cdots & \mathbf{P}_{BN}^h & \mathbf{0} \\ \mathbf{0} & \mathbf{0} & \mathbf{0} & \cdots & \mathbf{0} & \mathbf{P}_{BN}^e \end{bmatrix} \quad (2)$$

where h and e refer to LSE and LSM modes respectively. $\mathbf{H}$ is the E-field mode matching matrix which represents the coupling between the modes in the large guide and those of the N-furcated guide. $\mathbf{P}_A^h$, $\mathbf{P}_A^e$, $\mathbf{P}_{Bi}^h$, and $\mathbf{P}_{Bi}^e$ for i=1,2,3.....N, are diagonal matrices whose diagonal elements are the powers carried by unit amplitude LSE and LSM modes in the various guides.

In view of [5] and after some manipulations, the transmission matrix of the N-furcated discontinuity can be determined in terms of the three basic matrices defined above for LSE and LSM excitation. The transmission matrix $\mathbf{T}^T$ of the overall discontinuity shown in Fig 3. can then be easily obtained by simple matrix multiplications.

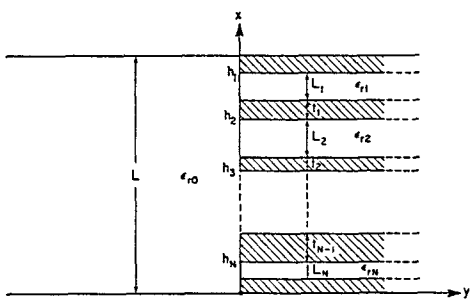

Fig. 2. An N-furcated waveguide junction.

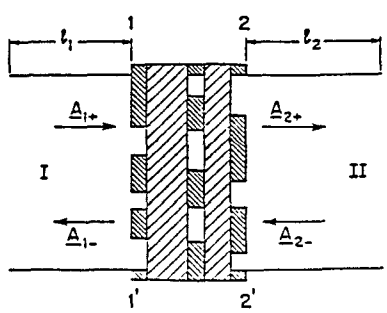

Fig. 3. A generalized discontinuity.

Having determined $\mathbf{T}^T$, application of the transverse technique yields the eigenvalue equation for the propagation constant β.

$$\begin{bmatrix} \mathbf{I} & -[\,\mathbf{T}_{11}^T - \mathbf{T}_{12}^T \mathbf{L}_2^- \mathbf{L}_2^-\,] \\ \mathbf{I} & \mathbf{L}_1^- \mathbf{L}_1^- [\,\mathbf{T}_{21}^T - \mathbf{T}_{22}^T \mathbf{L}_2^- \mathbf{L}_2^-\,] \end{bmatrix} \begin{bmatrix} \underline{A}_{1+} \\ \underline{A}_{2+} \end{bmatrix} = \mathbf{0} \quad (3)$$

where

$$\mathbf{L}_1^- = \begin{bmatrix} \mathbf{L}_1^{-\,h} & \mathbf{0} \\ \mathbf{0} & \mathbf{L}_1^{-\,e} \end{bmatrix}, \quad \mathbf{L}_2^- = \begin{bmatrix} \mathbf{L}_2^{-\,h} & \mathbf{0} \\ \mathbf{0} & \mathbf{L}_2^{-\,e} \end{bmatrix}. \quad (4)$$

$\mathbf{L}_1^{-\,h}$, $\mathbf{L}_1^{-\,e}$, $\mathbf{L}_2^{-\,h}$ and $\mathbf{L}_2^{-\,e}$ are diagonal matrices with diagonal elements given by

$$L_{1,nn}^{-\,h} = L_{1,nn}^{-\,e} = e^{-j\left[\omega^2\mu\epsilon - \left(\frac{n\pi}{L}\right)^2 - \beta^2\right]^{\frac{1}{2}} l_1} \quad (5)$$

$$L_{2,nn}^{-\,h} = L_{2,nn}^{-\,e} = e^{-j\left[\omega^2\mu\epsilon - \left(\frac{n\pi}{L}\right)^2 - \beta^2\right]^{\frac{1}{2}} l_2} \quad (6)$$

n=0,1,2... for LSE
n=1,2,3... for LSM

Solving for the eigenvector in (3) gives then the field amplitudes which are needed in the calculation of the characteristic impedance.

NUMERICAL RESULTS AND DISCUSSION

In Fig. 4 we show the effective dielectric constant $\epsilon_{eff} = (\beta/k_0)^2$ and the characteristic impedance Z versus frequency for unilateral finlines, with different slot widths and for metallizations of $t = 0$ and $t = 100\ \mu m$. Our results are in good agreement with those obtained by Kitazawa and Mittra [7], and our analysis can be used even for structures with infinitely thin fins. The results indicate that the metallization thickness has a significant effect on the characteristic impedance. Its effect however on the effective dielectric constant depends strongly on the slot width and is more pronounced for small slot widths.

Fig. 5 shows the normalized propagation constant of the dominant and the first higher order odd mode for groove depths of $e = 0$ and $e = 0.5\ mm$. It is observed that neglecting the mounting groove leads to a higher cutoff frequency and a lower value for the propagation constant. This in fact is expected and attributed to the part of the dielectric slab neglected in the mounting groove in the ideal case of $e = 0$. However, the effect of the groove on the dominant mode is significant when the first higher order mode starts to propagate. In addition, unlike the dominant mode's cutoff frequency, that of the first higher order mode decreases significantly when the mounting groove is used leading to a very large reduction in the single mode bandwidth.

Fig. 6 illustrates the effect of the mounting groove on the characteristic impedance. Our results confirm those recently published by Bornemann and Arndt [4]; the impedance follows the behavior of the dominant mode and starts to deviate from the ideal case ($e = 0$) only when the first higher order mode starts to propagate.

To demonstrate the fast convergence of the proposed analysis, Table I shows numerical results obtained for the propagation constant of the dominant and the first higher order modes and the characteristic impedance for a unilateral finline structure using different matrix sizes for the eigenvalue equation. A matrix size of (6x6) is quite enough to provide convergent results within 0.5 %.

In Fig. 7 the effect of the metallization thickness on the first four propagating modes in suspended microstrip lines is investigated. A noticeable effect is only observed on the propagation characteristic of the dominant mode. Finally, we consider in Fig. 8 the effect of the metallization thickness on the normalized propagation constant in a coplanar line on sapphire substrate. We also compare our results with those given in [9] for unshielded coplanar lines. Our results are obtained for the shielded structure shown in Fig. 8 with electric walls at $\pm b/2$ for the even mode and with magnetic walls at $\pm b/2$ for the odd mode. A good agreement is observed between the results for the dominant even mode. The reason however for the discrepancy between the results of the odd mode at low frequencies is that for this mode the fields are not tightly bound to the slots, and the waveguide walls may not be far enough from the slots at low frequencies to simulate the open structure.

CONCLUSIONS

The numerical results presented in this paper and the comparisons given with the other published data confirm the validity of the proposed analysis, and show that it is indeed a unified analysis. With a reasonably small matrix size, the achievable accuracy of the solution exceeds most engineering requirements.

REFERENCES

[1] L. P. Schmidt, T. Itoh and H. Hofmann, IEEE Trans. MTT-29, pp. 352-355, Apr. 1981.

[2] A. S. Omar and K. Schunemann, IEEE Trans. MTT-33, pp. 1313-1322, Dec. 1985.

[3] R. Vahldieck and J. Bornemann, IEEE Trans. MTT-33, pp. 916-926, Oct. 1985.

[4] J. Bornemann and F. Arndt, IEEE Trans. MTT-34, pp. 85-92, Jan. 1986.

[5] R. R. Mansour and R. H. MacPhie, IEEE Trans. MTT-34, pp. 1490 - 1498, Dec. 1986.

[6] R. R. Mansour and R. H. MacPhie, IEEE Trans. MTT-33, pp. 830-835, Sept. 1985.

[7] T. Kitazawa and R. Mittra, IEEE Trans. MTT-32, pp. 1484-1487, Nov. 1984.

[8] H. Hofmann, AEU Bd. 31. 1977, I, pp. 40 - 44.

[9] T. Kitazawa and Y. Hayashi, IEEE Trans. MTT-29, pp. 1035-1040, Oct. 1981.

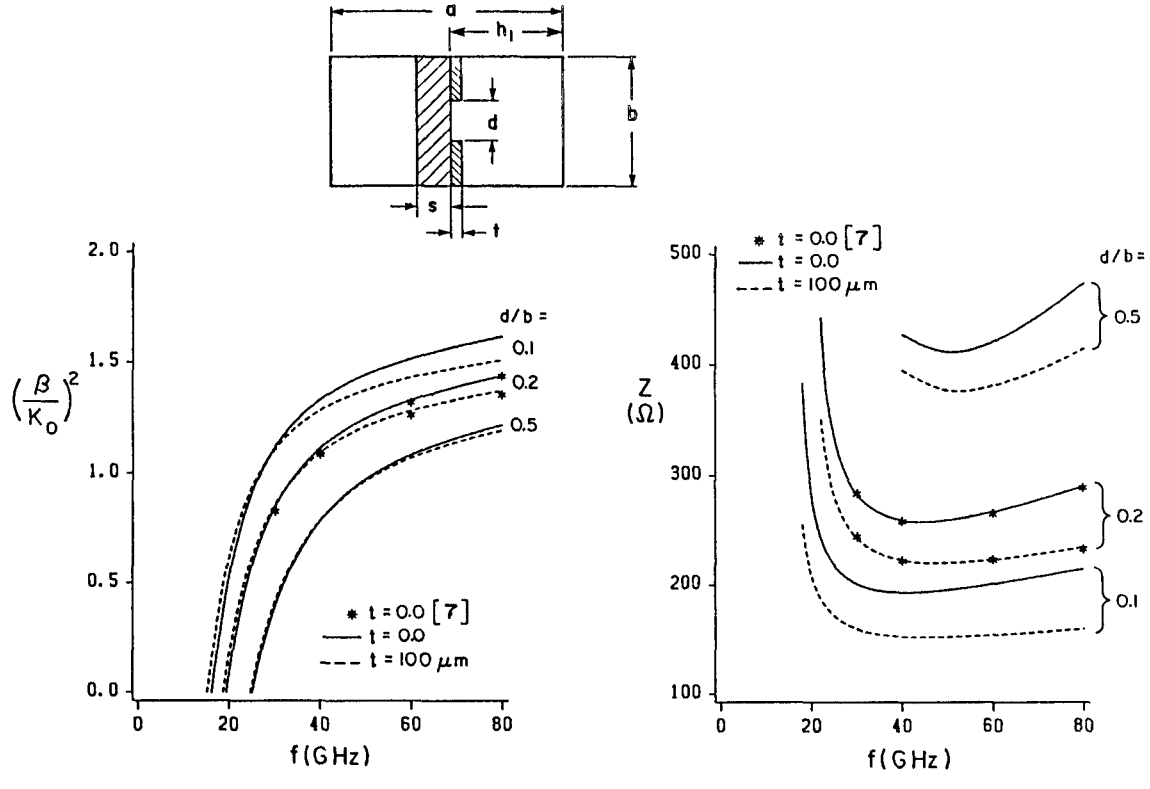

Fig. 4. Effective dielectric constant and characteristic impedance versus frequency in unilateral finlines with different values of slot width; $a=2b=4.7752\ mm$, $S=0.127\ mm$, $h_1=2.3876\ mm$, $\epsilon_r=3.8$.

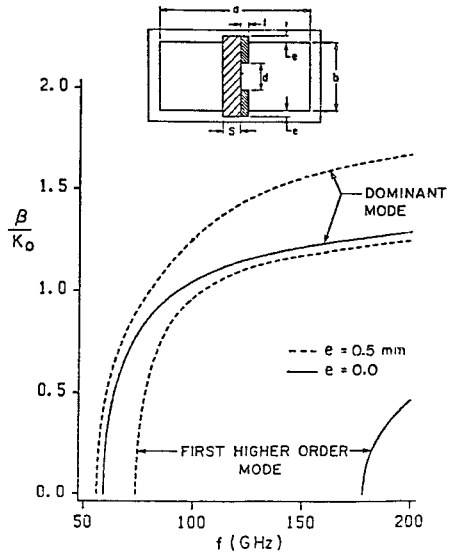

Fig. 5. Propagation characteristics of the dominant mode and first higher odd mode in a unilateral finline for $e=0$ and $e=0.5\ mm$; $a=2b=1.65\ mm$, $S=0.11\ mm$, $d=0.3\ mm$,

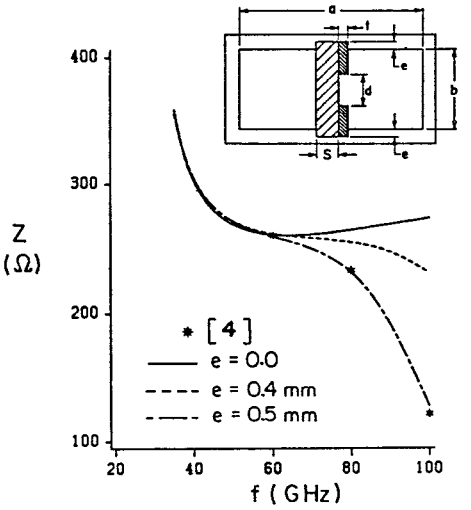

Fig. 6. Characteristic impedance of a unilateral finline versus frequency for different values of groove depth; $a=2b=3.1\ mm$, $S=0.22\ mm$, $d=0.4\ mm$, $\epsilon_r=3.75$, $t=5\ \mu m$.

TABLE I

The Normalized Propagation Constant and Characteristic Impedance of a Unilateral Finline Computed Using Different Matrix Sizes for the Eigenvalue Equation $a=2b=3.1$, $d=0.4\ mm$, $s=0.22\ mm$, $t=5\ \mu m$, $\epsilon_r=3.75$.

Dominant Mode, f = 60 GHz

Matrix Size	β/K_o	Impedance (Ω)
(4x4)	1.1855	257.03
(6x6)	1.1866	258.75
(8x8)	1.1866	260.10
(10x10)	1.1854	260.83

Dominant Mode, f = 100 GHz

Matrix Size	β/K_o	Impedance (Ω)
(4x4)	1.3326	269.64
(6x6)	1.3350	271.82
(8x8)	1.3356	273.48
(10x10)	1.3348	274.22

First Higher Order Mode, f = 100 GHz

Matrix Size	β/K_o
(4x4)	0.36959
(6x6)	0.36911
(8x8)	0.36879
(10x10)	0.36851

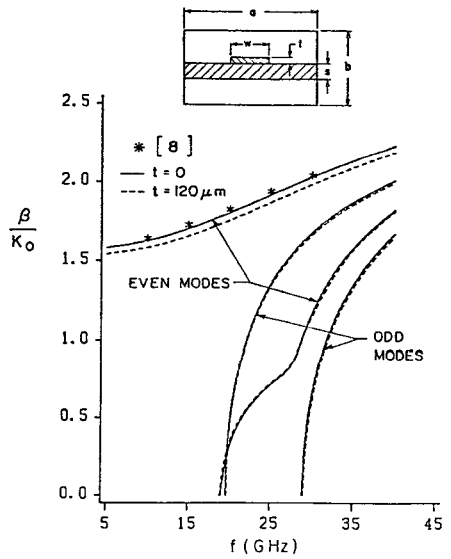

Fig. 7. Normalized propagation constant as a function of frequency for the suspended microstrip line; $a=2b=7.112\ mm$, $S=0.635\ mm$, $w=1.0\ mm$, $\epsilon_r=9.6$.

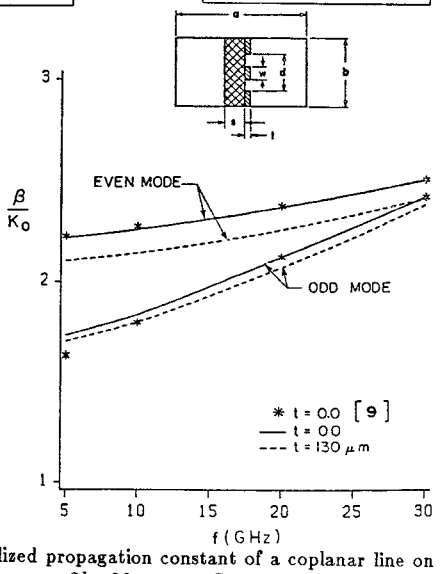

Fig. 8. Normalized propagation constant of a coplanar line on sapphire substrate; $a=2b=20\ mm$, $S=1.0\ mm$, $d=2.5\ mm$, $w=0.5\ mm$, (even mode) magnetic wall symmetry, (odd mode) electric wall symmetry.